

# Instability of the one-parameter renormalization group in the localization problem

V. E. Kwartsov and I. V. Lerner

*Institute of Spectroscopy, Academy of Sciences of the USSR*

(Submitted 27 August 1984; resubmitted 15 November 1984)

*Zh. Eksp. Teor. Fiz.* **88**, 1281–1299 (April 1985)

It is shown that the standard  $\sigma$  model used to derive the well-known one-parameter renormalization group (RG) equation describing quantum diffusion is unstable against the inclusion of a series of additional (microscopically derivable) vertices. The instability is due to the infinitely rapid growth of the additional RG charges, which affect the diffusion in a nonperturbative way, in the initial stage of the RG transformations.

## § 1. INTRODUCTION

The scaling theory of localization proposed by Abrahams, Anderson, Licciardello, and Ramakrishnan<sup>1</sup> has decisively altered the prevailing ideas about quantum diffusion of free particles in a disordered medium. The main conclusions of this theory include the absence of delocalized states in two-dimensional ( $d = 2$ ) systems and the absence of a sharp transition between localized and delocalized states for  $d > 2$ —contrary to Mott's idea that there is a minimum of the metallic conductivity.<sup>2</sup> These conclusions to a large extent rest on Thouless's hypothesis<sup>3</sup> that the only relevant scaling parameter in the localization theory is the conductance of the sample.

Thouless's hypothesis has found its most rigorous microscopic confirmation in the  $\sigma$ -model approach.<sup>4–11</sup> The use of the nonlinear tensor  $\sigma$  model<sup>12</sup> for describing quantum diffusion was proposed by Wegner.<sup>4</sup> This model was first derived microscopically (in different versions) by Efetov, Larkin, and Khmel'nitskiĭ<sup>5</sup> and by Wegner and Schäfer<sup>6</sup> and has since been derived by a number of other authors.<sup>7–11</sup> The  $\sigma$ -model approach has been used to obtain<sup>12,5,10</sup> a one-parameter renormalization-group (RG) equation which agrees in the region of weak disorder with the RG equation obtained qualitatively in Ref. 1. This approach has reproduced in a simple way the results of a direct summation of diagrams<sup>13</sup> and has also confirmed the conclusions of the one-parameter theory.<sup>1</sup>

In the present paper we show that the one-parameter description of quantum diffusion is unstable in a space of dimension  $d \geq 2$ . In a consistent microscopic description one must include an infinite number of relevant RG charges which affect the conductance of the system. These charges are due to the presence in the  $\sigma$  model of additional vertices proportional to higher powers of the matrix  $\Lambda$  which breaks the (global) symmetry of the model; this matrix was introduced in Wegner's original paper<sup>4</sup> and plays an extremely important role in the localization problem. (The additional vertices are obtained as small corrections in the usual microscopic derivation of the  $\sigma$  model in the quantum-diffusion problem.) The corresponding charges experience an infinitely rapid growth in the initial stage of the RG transformations, so that they must be taken into account even if their "bare" values are arbitrarily small.

We stress that such an instability is present only in the  $\sigma$  model describing the localization problem. In models de-

scribing other phase transitions (e.g., in the  $n$ -field model<sup>14</sup> or the  $CP^N$   $\sigma$  model<sup>15</sup>) the instability does not arise. In such models one can introduce additional vertices analogous to those under consideration, but they turn out to be irrelevant: the corresponding charges decay away under the RG transformations.

The fundamental distinction between the statistical models and the localization problem was recently demonstrated by Efetov,<sup>16</sup> who found an exact solution of the localization-theory  $\sigma$  model on the Bethe lattice. This model system exhibits a Mott transition between localized and delocalized states. Although this result is not directly relevant to a real physical system, the discrepancy with the conclusions of the scaling theory of localization<sup>1</sup> does not seem accidental. The instability of the one-parameter RG, as demonstrated in the present paper, shows that the nature of the localization for  $d \geq 2$  remains an open question.

## § 2. DESCRIPTION OF THE MODEL

The diffusion of noninteracting electrons in a disordered medium is described with the aid of the correlator

$$K(\mathbf{r}, \mathbf{r}'; \omega) = \langle G^R(\mathbf{r}, \mathbf{r}'; \varepsilon + \omega) G^A(\mathbf{r}', \mathbf{r}; \varepsilon) \rangle, \quad (1)$$

where  $G^{R(A)}$  is the retarded (advanced) Green function of an electron in a medium with randomly distributed impurities, and the angle brackets denote an averaging over the impurity distribution. By representing the Green functions as functional integrals one can perform in the very first step both the averaging over impurities and the integration of the "fast" electron variables which are irrelevant to the diffusion problem.

As a result, the calculation of correlator (1) reduces to evaluating the functional averages with a weight factor  $\exp(-F)$ , where  $F$  is the functional for the generalized nonlinear  $\sigma$  model<sup>4–11</sup>

$$F[Q] = \frac{\pi\nu}{8} \int d^d r \text{Sp} \{ \mathcal{D} (\nabla Q)^2 + 2i(\omega + i\delta) \Lambda Q \}. \quad (2)$$

Here  $\mathcal{D} = v_F l_0 / d$  is the diffusion coefficient ( $l_0 = v_F \tau_0$  is the mean free path,  $\tau_0$  is the time between elastic collisions),  $\nu$  is the electron density of states,  $\delta \rightarrow +0$ , and  $Q(\mathbf{r})$  is a  $2N \times 2N$  Hermitian matrix satisfying the conditions

$$Q^2 = 1, \quad \text{Sp} Q = 0. \quad (3)$$

The matrix elements of  $Q$  are the quaternions

$$Q_{ij} = Q_{ij}^a \hat{\tau}_a \quad (a=0, 1, 2, 3), \quad (4)$$

where  $\hat{\tau}_0$  is the  $2 \times 2$  unit matrix,  $\hat{\tau}_a = i\sigma_a$  ( $a = 1, 2, 3$ ), and the  $\sigma_a$  are Pauli matrices. In the case of potential scattering by impurities the  $Q_{ij}^a$  are real numbers; if in addition to the potential scattering there is a weak scattering by magnetic impurities (or in the presence of a weak external magnetic field), the  $Q_{ij}^a$  are complex numbers, and in the case of a spin-orbit interaction with impurities,  $Q_{ij}^0$  and  $Q_{ij}^3$  are real numbers and  $Q_{ij}^1$  and  $Q_{ij}^2$  are imaginary numbers<sup>1)</sup> (Ref. 5). It will sometimes be convenient to write the matrix elements of  $Q$  (and of other matrices) in the form  $Q_{ij} = Q_{ij}^{AB}$ , where  $A, B = 1, 2$  are block indices which arise on account of the averaging of the two different Green functions in correlator (1), and  $\alpha, \beta = 1, \dots, N$  are the replica indices. In the final results one should set  $N = 0$  in accordance with the usual replica method.<sup>17</sup>

It is very important in the following discussion that functional (2) contains a gradientless vertex  $\text{Sp}(\Lambda Q)$ , where the matrix  $\Lambda$  is

$$\Lambda = \begin{pmatrix} 1 & 0 \\ 0 & -1 \end{pmatrix} \otimes \delta_{\alpha\beta} \otimes \hat{\tau}_0.$$

The appearance of this vertex is due to the difference in the frequency dependences and analytic properties of the retarded and advanced Green functions in correlator (1).

In Refs. 12, 5, and 10 it was concluded that functional (2) is renormalizable. The only relevant RG charge turned out to be the dimensionless resistance  $t = (\pi\nu\mathcal{D}/8)^{-1}$ . In a space of dimension  $d = 2 + \varepsilon$  the Gell-Mann-Low equation for this charge in the one-loop approximation is of the form (in the replica limit  $N = 0$ )<sup>12,5</sup>:

$$d\tilde{t}/d\xi = -\varepsilon\tilde{t} - \alpha\tilde{t}^2 = \beta(\tilde{t}), \quad (5)$$

where  $\xi = \ln\lambda^{-1}$  is the logarithmic RG variable, and  $\tilde{t} = t/16\pi$ ; here

$$\tilde{t}_0 = (\pi\varepsilon_F\tau_0)^{-1} \ll 1 \quad (6)$$

is a small parameter of the theory and corresponds to a weak disorder. The coefficient  $\alpha$  depends on the pressure of scattering by magnetic or spin-orbit impurities in addition to ordinary potential scattering:

$$\alpha = \begin{cases} -1, & \text{potential scattering} \\ 0, & \text{magnetic case} \\ 1, & \text{spin-orbit scattering} \end{cases} \quad (7)$$

Equation (5) is valid for  $\tilde{t} \ll 1$ . In this limit it agrees with the equation proposed in the qualitative RG approach.<sup>1</sup> Since Eq. (5) was derived in a microscopic approach, it has served as the most rigorous justification for the qualitative approach.<sup>1</sup>

In the present paper we show that the picture based on the one-parameter RG is unstable. An infinite number of relevant RG charges, associated with the following additional vertices,<sup>2)</sup> arise in the system:

$$\Phi_n = \frac{\gamma_n}{t} \left( \frac{1}{\lambda\lambda_0} \right)^2 \int d^d r \text{Sp}(\Lambda Q)^n, \quad (8)$$

$$\Psi_{n1} = \frac{\Gamma_{n1}}{t} \int d^d r \text{Sp}(\Lambda Q)^n (\nabla Q)^2, \quad (9a)$$

$$\Psi_{n2} = \frac{\Gamma_{n2}}{t} \int d^d r \text{Sp}(\Lambda Q)^k \nabla Q (\Lambda Q)^{n-k} \nabla Q, \quad 1 \leq k \leq n-1, \quad (9b)$$

$$\Psi_{n3} = \frac{\Gamma_{n3}}{t} \int d^d r \text{Sp}(\Lambda Q)^{k-1} \Lambda \nabla Q (\Lambda Q)^{n-k-1} \Lambda \nabla Q, \quad 1 \leq k \leq n-1. \quad (9c)$$

These vertices are not "more nonlinear" than the original functional (2). The problem is that the interaction in the model is due to geometric restrictions (3) on the field  $Q(\mathbf{r})$ . Therefore, the functional integration should be carried out over independent components of the matrix  $Q$ . For this it is convenient to choose, for example, the following parametrization, analogous to that used in Ref. 11:

$$Q = \Lambda(1+W/2)(1-W/2)^{-1}, \quad W = \begin{pmatrix} 0 & B^+ \\ -B & 0 \end{pmatrix}. \quad (10)$$

Here  $B$  is an arbitrary  $N \times N$  matrix (whose elements, as in (4), depend on the type of scattering). Additional vertices (8) and (9), like the original vertex (2), contribute in the approximation quadratic in the independent variables  $W$ .

Let us first study the properties of the charges  $\gamma$  and  $\Gamma$  under the RG transformations and investigate their influence on the Gell-Mann-Low equation (6) for  $\tilde{t}$  (Sec. 3). We then present the scheme for deriving vertices (8) and (9) from the usual microscopic model of noninteracting electrons in a random field (Sec. 4). In Sec. 5 we discuss how the additional vertices contribute indirectly to the diffusion coefficient in the evaluation of correlator (1). In Sec. 6 we show that the instability in question is present only in the replica ( $N = 0$ ) limit of the investigated  $\sigma$  models (2)-(4) (or the equivalent supersymmetry  $\sigma$  models). A preliminary report of this study has been published elsewhere.<sup>20</sup>

### § 3. GROWTH OF THE CHARGES UNDER THE RG TRANSFORMATIONS

Let us consider the properties of the additional vertices (8) and (9) under the RG transformations in the standard scheme.<sup>14,5,10</sup> A field  $Q(\mathbf{r})$  satisfying conditions (3) is written in the form

$$Q = U^+ Q_0 U, \quad (11)$$

where the "fast" field  $Q_0(\mathbf{r})$  is written with the aid of parametrization (10), while the "slow" unitary matrices  $U(\mathbf{r})$  recast the "slow" field  $Q(\mathbf{r})$  in the form

$$\tilde{Q} = U^+ \Lambda U. \quad (12)$$

The functional  $\tilde{\mathfrak{F}}$ , describing the slow long-wavelength fluctuations is obtained by integrating over the fast variable  $Q_0(\mathbf{r})$ :

$$\tilde{\mathfrak{F}}[\tilde{Q}] = -\ln \int \exp(-\mathfrak{F}[Q]) DQ_0, \quad (13)$$

where  $\mathfrak{F} = F + \Phi + \Psi$  [see Eqs. (2), (8), and (9)].

It turns out that when vertices (8) and (9) are subjected to RG transformations (13), new auxiliary vertices are generated which should be included in the functional in order to ensure its renormalizability. Let us demonstrate this for the simplest—gradientless—vertices (8).

As a result of RG transformations (13) any  $\Phi_n$  vertex (8)

generates in the approximation linear in  $\gamma_n$  and  $t$  the following contribution to the functional describing the slow fluctuations (here  $d = 2$ ):

$$\delta\Phi_n[\tilde{Q}] = -\frac{\gamma_n \tilde{\xi}}{16\pi l_0^2} \left\{ \frac{n(n-1)}{2} \alpha \int d\mathbf{r} \text{Sp}(\Lambda Q)^n - \frac{n}{2} \sum_{k=1}^{n-1} \left[ \alpha \int d\mathbf{r} \text{Sp}(\Lambda Q)^{n-2k} + (\alpha^2 - 2) \Phi_n^k \right] \right\}. \quad (14)$$

(The derivation of this and other analogous expressions is outlined in Appendix 1). Here we generate the auxiliary vertices

$$\Phi_n^{h\infty} \int d\mathbf{r} \text{Sp}(\Lambda Q)^h \text{Sp}(\Lambda Q)^{n-h}. \quad (15)$$

One should also add these vertices to the functional, assuming that the "bare" values of the corresponding charges are equal to zero. Under the RG transformations vertices (15), in turn, contribute to the renormalization of the initial vertex  $\Phi_n$  and also generate auxiliary vertices containing products of three matrix traces.

By repeating this procedure the required number of times, we ultimately add to the functional all possible vertices of the form

$$\Phi_n^{(k_j)} = \frac{\gamma_n^{(k_j)}}{t} \frac{1}{(\lambda l_0)^2} \int d\mathbf{r} \prod_j \text{Sp}(\Lambda Q)^{k_j}, \quad (16)$$

where  $\{k_j\}$  is any set of whose numbers which satisfies the condition  $\sum k_j = n$ . We note that the number of necessary auxiliary vertices (16) (equal to the number of ways in which one can represent  $n$  in the form of a sum of natural numbers) grows extremely rapidly with increasing number ( $n$ ) of  $\Lambda$  matrices in the original additional vertices (8).

The functional including all the vertices (16) together with the original vertices (2) and (8) is formally renormalizable in the single-loop approximation. The RG equations (derived in Appendix 1) for the "vector"  $\gamma_n$ , whose components are all the charges  $\gamma_n^{(k_j)}$ , are conveniently written

$$d\tilde{\gamma}_n/d\tau = C\tilde{\gamma}_n, \quad (17)$$

where  $\tilde{\gamma}_n = \gamma_n \tilde{t}^{-1}$ , and  $\tau$ , with allowance for (6) and (7), is

$$\tau = \begin{cases} \ln(1 + \alpha \tilde{t}_0)^\alpha, & |\alpha| = 1 \\ -\tilde{t}_0 \tilde{\xi}, & \alpha = 0 \end{cases}, \quad (18)$$

Here  $C$ , the matrix of coefficients, depends on  $n$  and  $\alpha$  [i.e., on the type of scattering (7)] in an extremely complicated way, but its largest eigenvalue, which governs the growth of the charges  $\gamma_n$  in linear equations (17), nevertheless turns out to have a very simple dependence on these parameters (see Appendix 1):

$$\lambda_{\max} = \begin{cases} n^2 - n, & \alpha = 0, -1 \\ 1/2(n^2 - n), & \alpha = 1 \end{cases}. \quad (19)$$

Thus the initial growth of the charges  $\gamma_n$  under the RG transformations is described by the following formula:

$$\gamma_n \propto \exp[(n^2 - n)\tau] \propto \exp[(n^2 - n)\tilde{t}_0 \tilde{\xi}]. \quad (20)$$

It turns out (see Appendix 2) that the RG equations for

the charges  $\Gamma_n$  associated with the gradient vertices (9a)–(9c) agree with equations (17) to within unimportant parameters, the charges associated with different vertices being renormalized independently of one another in the linear approximation. Therefore, in the initial stage of the RG transformations all the charges  $\Gamma_n$  (9a)–(9c) also grow in accordance with (20).

It will be shown in Sec. 4 that the bare values of the charges  $\gamma_n$  and  $\Gamma_n$  fall off with increasing  $n$ :  $\gamma_n^0 \sim \Gamma_n^0 \sim (\omega\tau_0)^n \ll 1$ . Nevertheless, for large enough  $n$  the renormalized values of the charge  $\gamma_n$  and  $\Gamma_n$  reach a value  $\sim 1$  (regardless of their bare values) because of the  $n^2$  dependence in exponential law (20). For estimating the value of the renormalized charge it is convenient to set the parameter  $\xi$  equal to  $\xi_0 = \ln(\omega\tau_0)^{-1}$ . Then even in the region  $\tilde{t}_0 \xi \ll 1$  the charge

$$\gamma_n \sim (\omega\tau_0)^n \exp[(n^2 - n)\tilde{t}_0 \xi_0] \sim (\omega\tau_0)^{n(1 - n\tilde{t}_0)},$$

i.e., beginning with numbers  $n \gtrsim t_0^{-1}$ , all the charges grow without bound with decreasing frequency  $\omega$ .

This same conclusion is also valid in a space of dimension  $d > 2$ . Here one must only replace the parameter  $\tau$  in (20) by  $\tau_\varepsilon$  ( $\varepsilon = d - 2$ ):

$$\tau_\varepsilon = \begin{cases} \ln[1 + \alpha \tilde{t}_0 e^{-1}(1 - e^{-\varepsilon})]^\alpha, & |\alpha| = 1 \\ \tilde{t}_0 e^{-1}(1 - e^{-\varepsilon}), & \alpha = 0. \end{cases} \quad (21)$$

We see from expression (14) that equations of type (17) are formally related: any vertex  $\Phi_n$  contributes to the renormalization of the vertices containing a smaller number of matrices  $\Lambda$ . In the initial stage of the RG transformations (for  $\tau \propto \tilde{t}_0 \xi \rightarrow 0$ ) this contribution can be neglected (since the bare values of  $\gamma_n$  fall off with increasing  $n$ ); this corroborates Eq. (19). Further, by virtue of (20) the contribution of charges with larger  $n$  becomes dominant in the renormalization of any given charge. This promotes infinitely rapid growth of all charges  $\gamma$  for  $\tau \rightarrow +0$ .

The subsequent change of all the charges is due to the nonlinear character of the RG equations. It is important that the contributions nonlinear in  $\gamma$  and  $\Gamma$  to the RG equations are also proportional to  $n^2$  (see Appendix 2), i.e., have no influence (since the bare charges are small) on Eq. (20) for the growth of the charges in the initial stage of the RG transformations. In contrast, the corrections nonlinear in  $\tilde{t}$  (the many-loop corrections) to the RG equations can be proportional to any power of  $n$ . However, as is shown in Appendix 2, the most dangerous many-loop corrections to the eigenvalues of matrix (17) are proportional to  $n^2(n\tilde{t})^k \tilde{t}$ . This means that in the domain of application of the perturbative RG approach ( $\tilde{t} \ll 1$ ) these corrections do not affect the growth law (20) of charges with indices  $n \gtrsim \tilde{t}^{-1}$  (the extra power of  $\tilde{t}$  in the many-loop corrections ensures the necessary formal smallness). At the same time, for charges with indices  $n \gg \tilde{t}^{-1}$  the single-loop growth law (20) no longer applies. (This does not imply, of course, that the changes do not grow—we simply cannot describe their behavior in this approach even in the initial stages of the renormalization group). The growth of charges with indices somewhat greater than  $\tilde{t}^{-1}$  promotes the growth of all charges with smaller indices by virtue of the aforementioned coupling

between the equations. When these charges reach  $\sim 1$  the nonlinear corrections should be taken into account.

When the nonlinearity is taken into account, the RG equations for all the charges (including the "resistance"  $\tilde{r}$ ) become coupled. Therefore, the inclusion of any of the new charges will cause an avalanche-like growth of all such charges. In this case it would not appear feasible to obtain information on the change in the charges in the nonlinear regime, as this would require solving an infinite system of nonlinear RG equations.

We can nevertheless state definitely that all vertices (8) and (9) are relevant under the RG transformations, so that the fixed point  $\gamma = \Gamma = 0$  is unstable. The infinitely rapid growth of the charges in the initial stage of the RG transformations causes them to have a substantial effect on the renormalization of the dimensionless resistance: the simple equation (5) should be replaced by Eq. (A.11) (see Appendix 1). In Sec. 5, we show that these vertices also contribute directly to the diffusion coefficient.

#### § 4. DERIVATION OF ADDITIONAL VERTICES FROM THE MICROSCOPIC MODEL

The reasons why the  $\sigma$  model [Eqs. (2) and (3)] must be supplemented with vertices (8) and (9) in a consistent microscopic description can be illustrated as follows. When quantum corrections are ignored, the conductivity is described by the classical Drude formula:

$$\sigma(\omega) = ve^2 \mathcal{D} / (1 - i\omega\tau). \quad (22)$$

The standard  $\sigma$  model (2) cannot reproduce the frequency dependence in (22): the only  $\omega$ -dependent term in (2) does not contribute to the diffusion coefficient (and remains unchanged under renormalization).

The problem is that small frequency corrections are neglected in the derivation of the  $\sigma$  model. Let us outline a consistent microscopic derivation of the model with allowance for the  $\omega$  corrections (for simplicity we shall restrict the discussion to the case of potential scattering,  $\alpha = -1$ ); this approach will give rise to vertices (8) and (9). We must take these vertices into account, of course, not in order to reproduce the Drude formula, but because of the extraordinarily rapid growth of the corresponding charges (Sec. 3). At the same time, formula (22), like the law of conservation of number of particles (Sec. 5), is a convenient test of the internal consistency of the theory.

Correlator (1), which describes the quantum diffusion of noninteracting electrons in a random potential, is conveniently written in the form

$$K(\mathbf{r}, \mathbf{r}'; \omega) = \frac{\tau_0^2}{4N^2 Z} \int \text{Sp} \left\{ \frac{\delta^2}{\delta h(\mathbf{r}) \delta h(\mathbf{r}')} \exp(-S[Q, h]) \right\} DQ \Big|_{h=0}^{N=0}, \quad (23)$$

where

$$Z = \int \exp\{-S[Q]\} DQ, \quad S[Q] = S[Q, h=0], \quad (24)$$

while the generating functional  $S[Q, h]$  is defined by the

expression

$$S[Q, h] = \frac{\pi\nu}{8\tau_0} \int d\mathbf{r} \text{Sp} Q^2(\mathbf{r}) - \ln \int \exp \left\{ i \int d\mathbf{r} \bar{\psi} G^{-1} \psi \right\} D\bar{\psi} D\psi. \quad (25)$$

The functional integration in (25) is over intermediate  $2N$ -component fermion fields ( $N$  is the number of replica components), while the matrix Green function  $G$  is

$$G(\mathbf{r}) = - \left[ \frac{1}{2m} \frac{\partial^2}{\partial \mathbf{r}^2} + \varepsilon_F + \frac{i}{2\tau_0} Q(\mathbf{r}) + \frac{1}{2} (\omega + i\delta) \Lambda - \frac{i}{2\tau_0} h(\mathbf{r}) \right]^{-1}. \quad (26)$$

The matrix structure of the auxiliary field  $h(\mathbf{r})$  is

$$h = \begin{pmatrix} 0 & h_0 \\ h_0^\tau & 0 \end{pmatrix} \otimes \hat{\tau}_0 + \begin{pmatrix} 0 & h_3 \\ -h_3^\tau & 0 \end{pmatrix} \otimes \hat{\tau}_3, \quad (27)$$

where  $h_0$  and  $h_3$  are arbitrary real  $N \times N$  matrices and  $h^T$  is the transposed matrix.

Correlator (23) with definition (24)–(27) is essentially the same as the correlator obtained in Refs. 5, 6 and 10 (the correlator in form (23) was derived in Ref. 18). We stress that expression (23) is formally exact.

For  $\omega = h = 0$  action (25) reaches a minimum for the class of spatially constant fields  $\bar{Q}_0$  satisfying condition (3).<sup>5,6</sup> In the case of slight disorder (6) the long-wavelength properties of the model are determined solely by the transverse fluctuations of the field  $Q(\mathbf{r})$  about the minimum,<sup>5,6</sup> i.e., one should take into account in the integral of (23) only fields  $Q(\mathbf{r})$  which satisfy condition (3). (In the present case of potential scattering, where the matrix (4) is quaternion-real, condition (3) defines the quaternion Grassmann manifold  $\text{Sp}(2N)/\text{Sp}(N) \times \text{Sp}(N)$ .)

To evaluate the hydrodynamic action  $\mathfrak{F}$  (usually called the effective free energy) we expand functional (25) in slow transverse fluctuations  $\delta Q = Q(\mathbf{r}) - \bar{Q}_0$  about the minimum:

$$\mathfrak{F}[Q] = \mathfrak{F}_0 + \sum_n \frac{(-1)^n}{(2\tau_0)^{2n}} \int \left[ \int d\mathbf{r} \bar{\psi} \delta Q \psi \right]^n D\bar{\psi} D\psi e^{iS_0}, \quad (28)$$

where

$$S_0 = \int d\mathbf{r} \bar{\psi} G_0^{-1} \psi, \quad (29)$$

and  $G_0$  is obtained from  $G$  (26) by replacing  $Q(\mathbf{r})$  with  $\bar{Q}_0$ . The Gaussian integration in (28) gives, in the usual way, a product of Green functions  $G_0$ .

The small parameter of expansion (28) is actually  $kl_0$ , where  $k^{-1}$  is the characteristic scale of spatial variations in the field  $Q(\mathbf{r})$ . For  $\omega = 0$  expansion (28) in the first nonvanishing order in  $kl_0$  gives the gradient term of the ordinary  $\sigma$  model (2).

To incorporate the  $\omega$  corrections the green functions  $G_0$  should be expanded in  $\omega\tau_0$  (we are assuming for now that  $h = 0$ ). We see from (26) that this expansion is simultaneously an expansion in the matrix  $\Lambda$ . To first order in  $\omega\tau_0$  this expansion gives the  $\omega$ -dependent term of the ordinary  $\sigma$  model (2). Further expansion in  $\omega$  gives rise to vertices (8) and (in conjunction with the expansion to second order<sup>3</sup>) in  $kl_0$  vertices (9). Thus the bare values of the charges  $\gamma_n$  and

$\Gamma_n$  at vertices containing  $n$  matrices  $\Lambda$  are proportional to  $(\omega\tau_0)^n$  (the numerical values of the bare coefficients and certain details of the derivation for  $n = 1, 2$  are given in Ref. 18).

We stress that if we were able to obtain (by some non-perturbative method, for example) arbitrarily small but  $\omega$ -independent values of any charges  $\gamma, \Gamma$ , then the one-loop law (19) would lead to unbounded growth of charges with any indices  $n$ , as the many-loop corrections are known to be negligible in the initial stage of the RG transformations.

## § 5. CONTRIBUTION OF ADDITIONAL VERTICES TO THE CORRELATOR

In this section we describe how the additional vertices (8) and (9) contribute directly to the diffusion coefficient and show that the presence of gradientless vertices (8) does not necessarily lead to nonconservation of particle number. To calculate the correlator (23) the generating functional (25) must be expanded up to terms quadratic in the auxiliary field  $h(\mathbf{r})$ . To this end, the Green functions that appear in (28) must be expanded in powers of  $h$ . When vertices (8) and (9) are neglected, only one  $h$  term in the generating functional is important:  $SphQ$ .

Vertices (8) and (9) are obtained as a result of expanding Green function  $G_0$  (expressions (26) for  $Q(\mathbf{r}) = \bar{Q}_0$ ) in powers of  $i\omega\tau_0\Lambda$ . With allowance for the field  $h$  the expansion is in powers of the combination  $i\omega\tau_0\Lambda + h$ . Therefore, in addition to vertices (8) and (9) one gets (to within numerical coefficients) the various  $h$  vertices obtained by replacing one or two matrices  $\omega\tau_0\Lambda$  by the matrix  $h$ . In addition, expansion in  $kl_0$  leads to the vertices containing  $\nabla h$  that can be obtained from (9) by the substitution  $\nabla Q \rightarrow \nabla h$ .

The evaluation of the correlator by the RG procedure reduces to the problem of calculating the correlator in the approximation of noninteracting fluctuational modes using the renormalized values of all the relevant charges instead of the bare values. In the situation under study this procedure should also include the renormalization of the coefficient in all the  $h$  terms. (This, of course, is equivalent to renormalizing the pre-exponential factor of correlator (23); this factor has an extremely complex structure when the  $\omega$  dependence is taken into account).

In the case of the  $\sigma$  model, where the interaction is determined by geometric restriction (3), the free-diffusion approximation corresponds to an expansion of all the vertices up to second order in the independent variables  $W$  of Eq. (10). The effective diffusion coefficient has the simplest dependence on the charges  $\Gamma$  (9) when all the  $h$  terms except  $SphQ$  are neglected. In this approximation correlator (23) has the usual diffusional form:

$$K(\mathbf{k}, \omega) = \frac{2\pi\nu}{\mathcal{D}_{eff}\mathbf{k}^2 - i\omega}, \quad (30)$$

where the renormalized diffusion coefficient  $\mathcal{D}_{eff}$  is

$$\mathcal{D}_{eff} = (2\pi^2\nu\tilde{\nu})^{-1} \left[ 1 + \sum_n (\Gamma_{n1} + \Gamma_{n2} - \Gamma_{n3}) \right]. \quad (31)$$

Thus vertices (9) not only change the form of the RG equation for  $\tilde{\nu}$  but also contribute directly to  $\mathcal{D}$ . Here the two

types of contribution do not cancel each other, and the RG equation for  $\mathcal{D}_{eff}$  depends substantially on  $\Gamma$ .

To describe the dependence of the diffusion coefficient on the gradientless vertices  $\Phi_n$  (8) one should take into account all the  $h$  and  $h^2$  vertices obtained from (8) by the substitution  $\omega\tau_0\Lambda \rightarrow h$ . The generating functional in the free-diffusion approximation is

$$S[Q, h] = -(\pi\nu/8) \sum_{\mathbf{k}} \{ (\mathcal{D}_{eff}\mathbf{k}^2 - i\omega Z) \text{Sp } W_{\mathbf{k}} W_{-\mathbf{k}} - \tau_0^{-1} (2X \text{Sp } h_{\mathbf{k}} \Lambda W_{-\mathbf{k}} - Y \text{Sp } h_{\mathbf{k}} h_{-\mathbf{k}}) \}. \quad (32)$$

Here  $X, Y$ , and  $Z$  are renormalization factors which depend on  $\xi = \ln\lambda^{-1}$ . The quantity  $Z$  is determined by the contribution of all vertices (8):  $Z \propto \sum \gamma_n n^2$ . Analogously,  $X$  or  $Y$  is determined by the contribution of all the vertices obtained from (8) by replacing one or two  $\Lambda$  matrices, respectively, by  $h$ . Then correlator (23) becomes

$$K(\mathbf{k}, \omega) = \frac{2\pi\nu X^2}{\mathcal{D}_{eff}\mathbf{k}^2 - i\omega Z} + 2\pi\nu\tau_0 Y. \quad (33)$$

In order to have conservation of particle number

$$K(0, \omega) = 2\pi\nu/(-i\omega), \quad (34)$$

it is necessary that the renormalization factors be related by

$$X^2 Z^{-1} = 1 + i\omega\tau_0 Y. \quad (35)$$

With allowance for (35) correlator (33) reduces to the ordinary diffusion form (30) with a diffusion coefficient

$$\bar{\mathcal{D}}_{eff} = \mathcal{D}_{eff} X^2 Z^{-2} \quad (36)$$

instead of  $\mathcal{D}_{eff}$ .

Relation (35) should be satisfied at all stages of the RG transformations. Its validity for the bare values of the coefficients  $X, Y$ , and  $Z$  is guaranteed by the aforementioned relation between the coefficients for the  $\omega$  and  $h$  vertices. This relation is maintained during the RG transformations on account of the special matrix structure (27) of the field  $h(\mathbf{r})$ . The corresponding RG equations are rather awkward and will not be given here (they are analogous to those derived in Appendix 1).

In deriving relations (31) and (36) we ignored the  $h$  vertices containing the gradients of the fields  $h$  and  $Q$ . When these vertices are taken into account the formula for the effective diffusion coefficient depends on two more renormalization factors. We shall not give this formula since the purpose of this section is to demonstrate the connection between vertices (8) and (9) and the effective diffusion coefficient  $\mathcal{D}_{eff}$ . To actually evaluate  $\mathcal{D}_{eff}$  in a perturbative RG approach involves the solution of an infinite system of nonlinear RG equations (or the equivalent nonlinear functional equations—see Appendix 1) and does not seem feasible.

## § 6. ABSENCE OF THE INSTABILITY IN THE STATISTICAL MODELS

We shall show that the instability described above is peculiar to the  $\sigma$  models which arise in the description of quantum diffusion and does not appear in the description of phase transitions in non-Abelian statistical models. As a

simple example let us consider the  $\mathbf{n}$  field model<sup>14</sup>:

$$F = \frac{1}{t} \int d\mathbf{r} (\nabla \mathbf{n})^2, \quad (37)$$

where the  $N$  component vector  $\mathbf{n}$  lies on a sphere  $S^{N-1}$ . For  $N > 2$  this  $\sigma$  model, like model (2)–(4) for  $\alpha = -1$ , is asymptotically free.<sup>14</sup> If this model is treated as the long-wavelength limit of a lattice magnet with an anisotropic interaction, then anisotropy terms analogous to the additional vertices (8) and (9) arise in the microscopic derivation. For example, the vertex analogous to (9a) is written

$$\Psi_n = \frac{\Gamma_n}{t} \int d\mathbf{r} (\Lambda \mathbf{n})^n (\nabla \mathbf{n})^2, \quad (38)$$

where the vector  $\Lambda = (1, 0, \dots, 0)$ .

It turns out that the anomalous dimensionality  $t_0 \lambda_n / 8\pi$  of vertex (38) is always negative:

$$\lambda_n = -n^2 - n(N-2). \quad (39)$$

Consequently, the anisotropy terms (38) turn out to be irrelevant in the  $\mathbf{n}$ -field case. In the case of the  $CP^{N-1}$   $\sigma$  model<sup>15</sup> describing a system with an  $N$  component complex order parameter an analogous statement holds: the anomalous dimensionality of the anisotropy vertex introduced in the corresponding way is negative:

$$\lambda_n = -n^2 - n(N-1). \quad (40)$$

Let us now find out whether the additional vertices (8) and (9) affect the RG properties of  $\sigma$  model (2)–(4) for integer  $N$  (all the RG results given above referred only to the replica limit  $N = 0$ ). Let us focus for now on the case  $\alpha = 0$ , in which conditions (2)–(4) define the  $\sigma$  model on the complex Grassmann manifold  $U(2N)/U(N) \times U(N)$ . Let us consider the somewhat more general  $U(2N)/U(p) \times U(2N-p)$  Grassmann  $\sigma$  model [defined by conditions (2)–(4) with  $\text{Sp}Q = 2(N-p)$ ,  $1 \leq p \leq N$  in place of  $\text{Sp}Q = 0$ ]. The RG scheme for this model, which includes the additional vertices (8) and (9), is the same for arbitrary  $p$  as the scheme for  $p = N$  given in Sec. 3 and Appendix 1. The greatest eigenvalue, which describes the exponential growth of additional vertices (8) and (16) [or (9) and (A.1)], turns out to be independent of  $p$  and equal to

$$\lambda_{\max} = n^2 - n(2N+1). \quad (41)$$

However, by virtue of the obvious isomorphism (for  $p = 1$ )  $U(2N)/U(1) \cdot U(2N-1) \approx CP^{2N-1}$  (Ref. 19), this formula at first glance is inconsistent with formula (40) for the  $CP^{N-1}$  model [while for  $N = 1$ , by virtue of the isomorphism  $CP^1 \approx S^2$ , formula (41) is also inconsistent with formula (39) for the case of the three-component  $\mathbf{n}$  field]. The inconsistency is, of course, illusory. Formula (41) gives the greatest eigenvalue of the matrix  $\mathbf{C}$  (17). It turns out, however, that for all natural numbers  $N$  the contributions  $\propto \exp(\lambda_{\max} \tilde{t}_0 \tilde{\xi})$  to the action cancel. Moreover, for  $p = 1$  the action contributions corresponding to all the eigenvalues of the matrix  $\mathbf{C}$  except the smallest cancel, and that eigenvalue is precisely what is given by formula (40).

The point is that the vertices (8) and (16) [or (9) and (A.1)] are not linearly independent for natural numbers  $N$  and  $p$ . To see this, we use the parametrization  $Q = \Lambda \exp W$ ,

where  $W$  is given by expression (10) with  $B$  being an arbitrary  $(2N-p) \times p$  matrix of complex numbers. Then for  $p = 1$  (and for any  $N$ ) we have  $\text{Sp}(\Lambda Q)^n = 2 \cos n\varphi + 2(N-p)$  (where  $\varphi^2 = B^+ B$ ), from which it is clear that vertices (16) and (8) are linearly dependent. The coefficients in the linear combinations are such that the action contributions proportional to the exponentials containing the extra [as compared with (40)] eigenvalues cancel.

For  $p > 1$  the contributions of all the eigenvalues no longer cancel. For stability of the model it is sufficient that the exponentials with positive arguments cancel. By virtue of formula (41), vertices with fixed "anisotropy order"  $n$  can be dangerous only for a model with  $N \leq n/2$ . Let us consider for this case the action contribution that is quadratic in  $W$ , assuming the charges of all the other vertices are renormalized:

$$\gamma_n = \sum_i c_i \mathbf{X}_i \exp(\lambda_i \tau)$$

( $\mathbf{X}_i$  is the eigenvector of matrix (17) corresponding to eigenvalue  $\lambda_i$ ). The contribution of the vertices containing the product of  $l$  matrix traces is proportional to  $N^{l-1}$ . Consequently, for any exponential there arises an  $\mathbf{X}_i$ -dependent polynomial of degree  $n-1$  in  $N$ . Direct evaluation for several  $n$  shows that the polynomials corresponding to all the eigenvalues except the smallest go to zero for  $N = 1, 2, \dots, m_\lambda$ , with  $m_{\lambda_{\max}} > n/2$  (the particular number of natural roots of the polynomial  $m_\lambda$  also depends on  $p$  and  $n$ ). The action contributions corresponding to certain eigenvalues cancel. In particular, for any natural  $N$  and  $p$  the growing action contributions corresponding to positive eigenvalues cancel. There is a similar cancellation for natural  $N$  and  $p$  in the quaternion Grassmann  $\sigma$  models [ $\alpha = \pm 1$ , see (7)]. It is natural to assume that such cancellations will also occur for any anisotropy order  $n$ .

We stress that in the replica limit  $N = 0$  (or in the equivalent supersymmetry approach)<sup>10,11</sup> such cancellations do not occur: only vertices (8) and (9) contribute directly to the action (to second order in  $W$ ), since the contributions of the auxiliary vertices (16) and (A.1) are proportional to  $N$  (or are identically zero in the supersymmetry approach).

## § 7. CONCLUSION

The main result of this paper is that the one-parameter RG for describing the quantum diffusion of noninteracting particles is unstable. The instability arises because the additional vertices (8) and (9) introduced into the standard  $\sigma$  model (2)–(4) turn out to be relevant under the RG transformations. Despite the small bare values of the corresponding charges, they can grow (within the limits of the approach used here) to values  $\sim 1$ , whereupon they substantially influence the diffusion. The diffusional behavior is ultimately described by a system (in essence infinite) of nonlinear RG equations that cannot be solved directly.

The instability is peculiar to the theory of localization. It appears only in the replica ( $N = 0$ ) limit of the  $\sigma$  models defined on Grassman manifolds (3) and (4) or in the  $\sigma$  models defined on the supersymmetry Grassman manifolds (the two descriptions are equivalent in a perturbative RG approach to

localization theory). No such instability appears in the description of phase transitions in non-Abelian statistical models (the  $\mathbf{n}$  field model, the  $CP^N$   $\sigma$  model). When these models are treated using ordinary perturbation theory (expanding in  $t_0\xi$ ) the difference between them does not show up. With allowance for the  $\sigma$  corrections in the theory of quantum diffusion (or the corrections in powers of the anisotropy coefficient in the case of magnets) the leading logarithms to highest orders in  $t_0$  no longer cancel, and asymptotic series with rapidly growing coefficients appear. These series are essentially the same in diffusion theory as in the statistics of magnets except for the signs of individual terms. The RG procedure can be regarded as the partial summation of these series. Formula (39) shows that the terms cancel one another in the case of magnets but not [by virtue of (19) and (20)] in the theory of localization.

The instability of the RG against the inclusion of additional charges does not mean that including them will appreciably alter the conductivity in the region  $t_0\xi \ll 1$ . The infinitely rapid growth of the charges at  $t_0\xi \rightarrow 0$  may indicate that the bare value of the "resistance"  $t_0$  depends on the physical (renormalized) value  $t$  in a nonanalytic way. Then in the region  $t_0\xi \sim 1$  the picture should be qualitatively different from the predictions of the one-parameter theory.

We sincerely acknowledge many discussions with V. M. Agranovich, A. I. Larkin, Yu. E. Lozovik, D. E. Khmel'nitskiĭ, and V. I. Yudson. We are especially grateful to K. B. Efetov and V. V. Lebedev for many constructive comments.

## APPENDIX 1

Here we outline the RG transformations of the additional vertices (8) and (9) in the linear approximation in the charges  $\gamma$  and  $\Gamma$ . In this approximation the charges corresponding to the four types of vertices (8) and (9a)–(9c) are renormalized independently of one another, as will become clear below. We give the derivation of the RG equations only for the charges corresponding to vertices (8) and (9a). The RG equations for the charges  $\Gamma_{n2}$  and  $\Gamma_{n3}$  differ only in an inessential way from the equations shown.<sup>4)</sup>

To ensure renormalizability one should include a number of auxiliary vertices in the functional in addition to (8) and (9a). In the case of gradientless vertex (8) the auxiliary vertices are given by (16). The renormalization of vertex (9a) (simply denoted  $\Psi_n$  in this Appendix) generates auxiliary vertices with the structure

$$\Psi_n^{(k_j)} = \Gamma_n^{(k_j)} t^{-1} \int d\mathbf{r} \psi_{k_1}(\varphi_{k_2}, \dots, \varphi_{k_j}), \quad (\text{A.1})$$

where  $\{k_j\}$  is a set of positive whole numbers whose sum is equal to  $n$ , while the densities of functionals (8) and (9a) for  $n = k$  are

$$\varphi_k = \text{Sp}(\Lambda Q)^k, \quad \psi_k = \text{Sp}(\Lambda Q)^k (\nabla Q)^2. \quad (\text{A.2})$$

Let us consider the change in the following functional under the RG transformations:

$$\mathfrak{F} = F + t^{-1} \Theta \equiv \int d\mathbf{r} f(\mathbf{r}), \quad (\text{A.3})$$

where  $F$  is the original functional (2) and  $\Theta t^{-1}$  is the sum of

all vertices (9a), (A.1) and (8), (16) in which the number ( $n$ ) of  $\Lambda$  matrices does not exceed a certain  $m$ . It is convenient to represent the density  $f$  of functional (A.3) in the form

$$f(\mathbf{r}) = t^{-1} [f(\mathbf{r}) + \theta(\mathbf{r})],$$

where  $f(\mathbf{r}) \equiv \psi_0(\mathbf{r})$  is the density of the gradient part of the original functional (2), and

$$\theta(\mathbf{r}) = \theta[\psi_1, \dots, \psi_m, \varphi_1, \dots, \varphi_m]$$

is the density of the functional  $\Theta[Q, \Lambda]$  [including the gradientless part of functional (2)] in implicit form.

To carry out the RG transformations (13) one should write the field  $Q(\mathbf{r})$  in form (11) and expand the rapid fields  $Q_0(\mathbf{r})$  in the independent variables  $W$  of Eq. (10). Then the evaluation of continuum integral (13) reduces to the problem of evaluating the functional averages with weight  $\exp(-F_0)$  (these averages are denoted below by the symbol  $\langle \dots \rangle_0$ ), where

$$F_0 = -\frac{1}{t} \int d\mathbf{r} \text{Sp}(\nabla W)^2 \quad (\text{A.4})$$

is the part of functional (2) that is quadratic in  $W$  and does not contain the slow variable  $\tilde{Q}(\mathbf{r})$  [Eq. (12)]. We note that upon substitution (10) the Jacobian of the change of variable from  $Q_0(\mathbf{r})$  to  $W(\mathbf{r})$  in integral (13) is equal to unity in the replica limit  $N = 0$ . Here we are discussing the RG transformations only in this limit.

Evaluations in the one-loop (linear in  $t$ ) approximation should be done by expanding functional (A.3) to terms of second order in  $W$ . Here the contribution to the renormalized functional  $\tilde{\mathfrak{F}}$  describing the slow fluctuations is given by the following expression:

$$\tilde{\mathfrak{F}} = \tilde{\mathfrak{F}}_0 + \langle \Theta_2 \rangle_0 - \langle \Theta_0 F_2 \rangle_0. \quad (\text{A.5})$$

Here we have made use of the fact that upon explicit separation of the fast and slow fields functional (A.3) decomposes into four parts:

$$\mathfrak{F} = \tilde{\mathfrak{F}}_0 + \mathfrak{F}_0 + \mathfrak{F}_1 + \mathfrak{F}_2, \quad (\text{A.6})$$

where  $\tilde{\mathfrak{F}}_0$  is equivalent to the functional  $\tilde{\mathfrak{F}}$  in terms of the slow variables  $\tilde{Q}$ , and  $\mathfrak{F}_j$  contains  $2 - j$  gradients of the fast variable  $W$ . In (A.5) allowance is made for the fact that  $F_1 \equiv 0$  in the approximation to second order in  $W$  if the gauge of the matrix  $\mathbf{A}_{\alpha\beta}^{AB}$  is chosen such that its block diagonal elements are equal to zero:  $\mathbf{A}^{11} = \mathbf{A}^{22} = 0$ .<sup>10,11</sup> Here  $\mathbf{A} = \nabla U U^+$  is the matrix in terms of which the gradients of the slow field are expressed:  $\nabla \tilde{Q} = U^+ [\Lambda, \mathbf{A}] U$ . All the expressions simplify considerably in this gauge since  $\{\Lambda, \mathbf{A}\} = 0$ .

The density of functional  $\Theta$  after expansion to second order in  $W$  is represented in the form

$$\theta_0 = \sum_{k=1}^n \frac{\partial \theta}{\partial \psi_k} (\delta^{(2)} \psi_k)_0, \quad (\text{A.7})$$

$$\begin{aligned} \theta_2 = & \sum_{k=1}^n \left\{ \frac{\partial \theta}{\partial \psi_k} (\delta^{(2)} \psi_k)_2 + \frac{\partial \theta}{\partial \varphi_k} \delta^{(2)} \varphi_k \right\} \\ & + \sum_{l+h \leq n} \left\{ \frac{1}{2} \frac{\partial^2 \theta}{\partial \varphi_l \partial \varphi_h} \delta^{(1)} \varphi_l \delta^{(1)} \varphi_h \right. \\ & \left. + \frac{\partial^2 \theta}{\partial \varphi_l \partial \psi_k} \delta^{(1)} \varphi_l (\delta^{(1)} \psi_k)_2 \right\}. \end{aligned} \quad (\text{A.8})$$

Here the superscripts (1) and (2) indicate the number of  $W$  matrices in the given variation, and the subscripts  $j = 0$  or  $j = 2$  on the variation  $\delta\psi$  gives the number of matrices  $A$  in it [ $2 - j$  is the number of gradients of the fast variable according to classification (A.6)]:

$$\begin{aligned} \delta^{(1)}\varphi_n &= n \operatorname{Sp} P^n W, \quad P \equiv \Lambda \tilde{Q}, \\ \delta^{(2)}\varphi_n &= \frac{n}{2} \sum_{k=1}^n \operatorname{Sp} P^{n-k} W P^k W, \\ (\delta^{(1)}\psi_n)_0 &= 0, \quad (\delta^{(2)}\psi_n)_0 = -\operatorname{Sp} P^n (\nabla W)^2; \\ (\delta^{(1)}\psi_n)_2 &= -4 \sum_{k=0}^n \operatorname{Sp} P^k W P^{n-k} A^2 + 2 \operatorname{Sp} [W, A^2] P^n, \\ (\delta^{(2)}\psi_n)_2 &= -4 \sum_{k+l \leq n} \operatorname{Sp} P^k W P^l W P^{n-k-l} A^2 \\ &+ 2 \sum_{k=0}^n \operatorname{Sp} P^k W P^{n-k} [W, A^2] + \operatorname{Sp} P^n \{W, A\}^2. \end{aligned} \quad (\text{A.9})$$

The usual RG equation (5) is obtained by evaluating the average  $\langle F_2 \rangle_0$  instead of (A.6). Evaluating this average in the usual way (see Refs. 5 and 18) together with average (A.6), we find after substituting expressions (A.7)–(A.10) into these averages that Eq. (5) becomes

$$\frac{d\tilde{r}^{-1}}{d\tilde{\xi}} = \alpha + \alpha \sum_{n \geq 1} n \frac{\partial \theta}{\partial \psi_{2n}} \Big|_{\varphi=\psi=0} + 2 \sum_{n \geq 1} n^2 \frac{\partial^2 \theta}{\partial \varphi_n \partial \psi_n} \Big|_{\varphi=\psi=0}. \quad (\text{A.11})$$

The bare values of the  $\theta$  terms in (A.11) are small since  $\gamma$  and  $\Gamma$  are small. Therefore, in the initial stage of the RG one can as before use Eq. (5) instead of (A.11). Then the RG equations for the function  $\theta = \tilde{r}^{-1}$ , obtained from (A.6) when (A.7)–(A.10) are taken into account becomes linear with respect to the variable  $\tau$  [see formulas (18) and (21)] and assumes the form (in the replica limit  $N = 0$ ):

$$\begin{aligned} -\frac{\partial \tilde{\theta}}{\partial \tau} &= \sum_{n \geq 1} \left\{ \frac{\partial \tilde{\theta}}{\partial \varphi_n} \left[ \frac{1}{2} \alpha n (n-1) \varphi_n + \frac{n}{2} \sum_{k=1}^{n-1} ((2-\alpha^2) \varphi_{n-k} \varphi_k - \alpha \varphi_{|n-2k|}) \right] \right. \\ &+ \frac{\partial \tilde{\theta}}{\partial \psi_n} \left[ \frac{1}{2} \alpha n (n-1) \psi_n + \sum_{k=1}^{n-1} \left( (n-k) (2-\alpha^2) \psi_{n-k} \varphi_k - \frac{\alpha n}{2} \psi_{|n-2k|} \right) \right] \\ &+ \sum_{k=1}^{n-1} \left[ 2(n-k) k \frac{\partial^2 \tilde{\theta}}{\partial \varphi_k \partial \psi_{n-k}} (\psi_n - \psi_{|n-2k|}) \right. \\ &\left. \left. + (n-k) k \frac{\partial^2 \tilde{\theta}}{\partial \varphi_k \partial \varphi_{n-k}} (\varphi_n - \varphi_{|n-2k|}) \right] \right\}. \end{aligned} \quad (\text{A.12})$$

Illustrative formula (14) given in the main text is obtained from the first line of formula (A.12) if just the  $\Phi_n$  vertex (8) is substituted in instead of the functional.

For relatively small  $n$  it is convenient to seek the solution of equations (A.12) after expressing the functional  $\Theta$  explicitly in the form of a sum of all the vertices (8), (9a), (16), and (A.1). In this case Eq. (A.12) breaks up (in the linear approximation under consideration) into independent systems of ordinary linear differential equations for the charges  $\gamma_n^{(k_j)}$  and  $\Gamma_n^{(k_j)}$ . The first of these is Eq. (17) in the main text, and the second is written symbolically as

$$d\tilde{\Gamma}_n/d\tau = \mathbf{D}^{(n)} \tilde{\Gamma}_n. \quad (\text{A.13})$$

Here  $\tilde{\Gamma}_n = \Gamma_n \tilde{t}^{-1}$ , where  $\Gamma_n$  is the vector with components  $\Gamma_n^{(k_j)}$ , with

$$\sum_j k_j = n.$$

Matrices  $\mathbf{C}^{(n)}$  and  $\mathbf{D}^{(n)}$  are found directly by substituting  $\Theta$  in the form of a sum of all vertices containing  $n$  matrices  $A$  in Eq. (A.12). For  $n = 1$  we have for these "matrices"  $\mathbf{D}^{(1)} = \mathbf{C}^{(1)} = 0$ .

For  $n = 2$  the density  $\tilde{\theta}$  of functional  $\tilde{\Theta}$  is

$$\tilde{\theta} = \gamma_2 \varphi_2 + \gamma_{11} \varphi_1 \varphi_1 + \Gamma_2 \psi_2 + \Gamma_{11} \psi_1 \varphi_1$$

and the matrices  $\mathbf{D}^{(2)}$  and  $\mathbf{C}^{(2)}$  coincide:

$$\mathbf{D}^{(2)} = \mathbf{C}^{(2)} = \begin{vmatrix} -\alpha & -2 \\ \alpha^2 - 2 & 0 \end{vmatrix}. \quad (\text{A.14})$$

For  $n = 3$  the density of functional  $\Theta$  is

$$\begin{aligned} \tilde{\theta} &= \gamma_3 \varphi_3 + \gamma_{21} \varphi_2 \varphi_1 + \gamma_{111} (\varphi_1)^3 + \Gamma_3 \psi_3 + \Gamma_{21} \psi_2 \varphi_1 \\ &+ \Gamma_{12} \psi_1 \varphi_2 + \Gamma_{111} \psi_1 (\varphi_1)^2 \end{aligned}$$

and the dimensionality of matrices  $\mathbf{C}^{(3)}$  and  $\mathbf{D}^{(3)}$  do not coincide. If the components of the vector  $\Gamma$  are chosen in the form  $(\Gamma_3, \Gamma_{21} + \Gamma_{12}, \Gamma_{111}, \Gamma_{21} - \Gamma_{12})$ , then

$$\mathbf{D}^{(3)} = - \begin{vmatrix} 3\alpha & 4 & 0 & 0 \\ 3(2-\alpha^2) & \alpha & 6 & 0 \\ 0 & 2-\alpha^2 & 0 & 0 \\ 2-\alpha^2 & 0 & 2 & \alpha \end{vmatrix}, \quad (\text{A.15})$$

and the matrix  $\mathbf{C}^{(3)}$  is the  $3 \times 3$  matrix on the upper left-hand corner of the matrix  $\mathbf{D}^{(3)}$ .

One is readily convinced by a direct calculation that the largest eigenvalues of matrices (A.14) and (A.15) are described by formula (19). Here all the eigenvalues of the matrix  $\mathbf{D}^{(3)}$  are integers, and the additional (in comparison with the matrix  $\mathbf{C}^{(3)}$ ) eigenvalue is negative. These regularities per-



sist at larger  $n$  as well: all the eigenvalues of the matrix  $\mathbf{C}^{(n)}$  are integers, this matrix being a diagonal block of the matrix  $\mathbf{D}^{(n)}$ , and the additional eigenvalues of the latter are negative.<sup>4)</sup> Thus the RG equations (17) and (A.13) for vectors  $\gamma$  and  $\Gamma$  agree to within irrelevant combinations of auxiliary charges  $\Gamma_n^{[k]}$ .

Law (19) for the largest eigenvalue of the matrix  $\mathbf{C}^{(n)}$  was checked by direct calculation all the way up to  $n = 7$  ( $\mathbf{C}^{(7)}$  is a  $15 \times 15$  matrix). We shall show<sup>5)</sup> that the asymptotic behavior of the largest eigenvalue of the matrix  $\mathbf{D}^{(n)}$  (or  $\mathbf{C}^{(n)}$ ) for  $n \gg 1$  is also described by  $\lambda_{\max} \sim n^2$ .

We write functional  $\Theta$  as a sum of gradient vertices (9a) and (A.1) each containing  $n$  matrices  $\Lambda$ , and we write the density of the functional in the form

$$\theta = \sum_{n^{-1} \leq x_i \leq 1} \Gamma(\tau; x_0, x_1, \dots, x_l) \psi(x_0) \varphi(x_1) \dots \varphi(x_l) \delta_{x_{i+1}}. \quad (\text{A.16})$$

Here the sets of variables  $\{\psi_k\}$  and  $\{\varphi_k\}$  ( $1 \leq k \leq n$ ) (A.2) have been replaced by functions  $\psi(x_0)$  and  $\varphi(x_i)$  of the discrete parameter

$$x = k/n, \quad (\text{A.17})$$

which runs over values from  $n^{-1}$  to 1. The discrete set of charges  $\Gamma_n^{[k]}$  has been written as a function  $\Gamma(\tau; x_0, x_1, \dots, x_l)$  which is specified at a discrete set of points  $\{x_i\}$ , where  $l$  is a rather large ( $\gg n$ ) fixed number that is formally independent of  $n$ , since the condition  $\sum k_j = n$  is taken into account by the Kronecker delta in (A.16).

The interval between adjacent values of the discrete variable  $x_i$  is  $\Delta x = 1/n$ . For  $n \gg 1$  the sum over  $x_i$  can be replaced by an integral:

$$\sum_{n^{-1} \leq x_i \leq 1} (\dots) \rightarrow n \int_0^1 dx_i (\dots). \quad (\text{A.18})$$

Here the Kronecker delta goes over to the  $\delta$  function:

$$\delta_{x_{i+1}} \rightarrow \frac{1}{n} \delta\left(\sum x_i - 1\right). \quad (\text{A.19})$$

As a result, the density of the functional [Eq. (A.16)] is now written

$$\theta = \theta^* n^{l-1} = n^{l-1} \int_0^1 dx_0 \dots \int_0^1 dx_l \Gamma(\tau; x_0, x_1, \dots, x_l) \times \psi(x_0) \varphi(x_1) \dots \varphi(x_l) \delta\left(\sum_{i=0}^l x_i - 1\right), \quad (\text{A.20})$$

where the functional  $\theta^*$  does not depend explicitly on  $n$ .

Expression (A.21) should be substituted into (A.12) (where the last terms in every line, which do not conserve  $n$ , have been discarded), which must also be converted from the discrete to the continuous description. Here the partial derivatives in (A.12) go over to the vibrational derivatives in accordance with the rules

$$\frac{\partial \theta}{\partial \varphi_m} \rightarrow \frac{1}{n} \frac{\partial \theta}{\delta \varphi(x)}, \quad \frac{\partial \theta}{\partial \psi_m} \rightarrow \frac{1}{n} \frac{\delta \theta}{\delta \psi(x)}, \quad (\text{A.21})$$

the correctness of which can be readily checked by comparing the formulas obtained by directly taking the derivatives  $\delta/\delta\varphi$  (or  $\delta/\delta\psi$ ) of (A.20) or by evaluating the corresponding partial derivative of (A.16) and then passing to the continuum limit using (A.17)–(A.19).

As a result, Eq. (A.12) is transformed into the following functional equation:

$$-\frac{\partial \theta^*}{\partial \tau} = \frac{n^2}{2} \int_0^1 dx \frac{\delta \theta^*}{\delta \psi(x)} \left\{ \alpha + (2 - \alpha^2) \int_0^x dy (x-y) \psi(x-y) \varphi(y) \right\} + 2n^2 \int_0^1 dx \int_0^1 dy xy \frac{\delta^2 \theta^*}{\delta \psi(x) \delta \varphi(y)} \psi(x+y) + \dots \quad (\text{A.22})$$

(Here we have explicitly written out the terms obtained by transforming the second and third lines of Eq. (A.12); analogous terms are obtained by transforming the first and fourth lines.) This equation can be written symbolically as

$$-\partial \theta^* / \partial \tau = n^2 G(\varphi, \psi),$$

where the functional  $G$  does not depend on  $n$ . It follows that  $\theta^*$  (and hence  $\Gamma$ ) does not depend on  $n^2 \tau$ , i.e., all the eigenvalues are proportional to  $n^2$ . Taken together with the direct calculations for  $n \leq 7$ , this proves formula (19).

We note that the  $n^2$  dependence is of a simple combinational origin: the order of magnitude of the relevant terms in (A.12) is determined by the number of permutations ( $C_n^2 \sim n^2$ ) of the two  $\mathcal{W}$  matrices in the functional  $\Theta_n$ . The above proof demonstrates that in the limit  $n \gg 1$  Eq. (A.12) is homogeneous in  $n$ , so that its eigenvalues have the same order of magnitude. These same combinatorial arguments are used below to estimate the  $n$  dependence of the contributions of higher orders in  $\Gamma$  and  $\tilde{t}$ .

## APPENDIX 2

Here we show that the contributions nonlinear in  $\Gamma$  and the multiloop contributions (nonlinear in  $\tilde{t}$ ) to the renormalized functional  $\mathcal{F}$  grow no faster than the linear contribution for  $n \rightarrow \infty$ , at least in the initial stage of the RG transformations. (If this were not the case, dependence (19) and (20), which were found in the linear approximation, would not apply even for  $\Gamma$ ,  $\tilde{t} \ll 1$ .)

The nonlinear contribution of order  $s$  (in  $\Gamma$ ) to the RG equation is given by the following averages:

$$\frac{(-1)^s}{s!} \langle \Theta_0^s F_2 \rangle_0 + \frac{(-1)^{s-1}}{(s-1)!} \langle \Theta_0^{s-1} \Theta_2 \rangle_0 + \frac{(-1)^{s-1}}{2(s-2)!} \langle \Theta_0^{s-2} \Theta_1^2 \rangle_0. \quad (\text{A.23})$$

The gradientless vertices (8) and (16) do not give a nonlinear (logarithmic for  $d = 2$ ) contribution to the RG equation, since  $\Theta_0$  and  $\Theta_1$  contain  $\nabla \mathcal{W}$  [see (A.7)–(A.10)].

Let us estimate the  $n$  dependence of the terms in (A.23). In  $\Theta_2$  one should choose the two matrices  $\mathcal{W}$  from an expression of the type  $[\Lambda \tilde{Q} (1 + \mathcal{W})]^n$ , which can be done in  $C_n^2$  ways—hence the proportionality to  $n^2$ . In  $\Theta_1$  (the explicit form of which is not given here), which contains one gradient

of the slow ( $\tilde{Q}$ ) variable and one gradient of the fast ( $W$ ) variable, one should choose only one matrix  $W$  in an expression of this type, while the second matrix  $W$  arises in the expansion of  $\nabla Q_0$  without any combinational coefficient; consequently,  $\Theta_1$  is proportional to  $n$ . Finally, in  $\Theta_0$ , which contains two gradients of the fast variable, there is no combinatorial freedom in the order in which the two  $W$  matrices are taken, i.e., no dependence on  $n$  arises. Therefore, the first term in (A.23) does not give rise to an important dependence on  $n$ , while the second and third give corrections to  $\lambda_{\max}$  that go as  $n^2 \Gamma^{s-1}$  and can be neglected as long as  $\Gamma \ll 1$ . All these qualitative arguments can be confirmed by a procedure analogous to the derivation of functional equations (A.22) in Appendix 1.

The multiloop corrections (in the approximation linear in  $\Gamma$ ) stem from the following averages ( $j \geq 0$ ):

$$\frac{(-1)^j}{j!} \left\langle \Theta_2 F_0'^j - \Theta_1 F_1 F_0'^j + \frac{1}{2} \Theta_0 F_1^2 F_0'^j - \Theta_0 F_2 F_0'^j \right\rangle_0. \quad (\text{A.24})$$

(Explicit expressions for  $F_0'$  and  $F_1$  are easily obtained with the aid of parametrization (10); they are given up to terms  $O(W^4)$  in Ref. 11.) Here the indices 0, 1, 2 correspond to classifications (A.6);  $F_0'$  contains not less than four, and  $F_1$  not less than three, matrices  $W$ . In actually evaluating the diagrams it is convenient to introduce explicitly the invariant counterterms for separating the fast variables from the slow and to use dimensional regularization of the ultraviolet divergences in accordance with the scheme of Ref. 10.

Examples of multiloop diagrams are given in Fig. 1. The important dependence on  $n$  is determined by the number of permutations of the  $W$  matrices in vertex  $\Theta_{2-j}$ : this is the number  $C_{n+m-j-1}^{m-j}$  of ways in which an expression of degree  $m-j$  in  $W$  can be obtained from  $[\Lambda \tilde{Q} (1 + W + W^2/2 + W^3/4 + \dots)]^n$ , where  $m$  is the number of lines leaving the vertex and  $j$  is the number of gradients of the fast variable in the vertex; for  $n \gg m$  this number varies as  $n^{m-j}$ .

Let us consider the diagrams corresponding to the first term in (A.24) [this is the only term which contributes to the renormalized gradientless vertices (8)]. At a fixed number  $m$  of lines leaving vertex  $\Theta_2$ , the smallest number of loops (i.e., the minimum possible power of the small parameter  $\tilde{t}$ ),  $l = m/2$ , is for diagrams of the type shown in Fig. 1a: they are proportional to  $n^m \tilde{t}_0^{m/2-1}$ . These diagrams, however, do not contribute to the Gell-Mann–Low equation. The reason is that in evaluating the  $l$ -loop contribution to the function  $\beta$  ( $\propto \tilde{t}_0^{-1}$ ) the bare values  $\tilde{t}_0$  and  $\Gamma_0$  of the charges in the diagram should be expressed in terms of the physical values of these charges to an accuracy  $\sim \tilde{t}_0^{l-2}$ . Then the diagrams of type a cancel with powers of diagrams having a smaller number of loops. This also applies to diagrams of type b and in general to all diagrams which “repeat” diagrams of lower orders (i.e., diagrams which can be cut into disconnected parts at a single junction point).

Since diagrams of type b need not be taken into account, the minimum possible number of loops at a fixed number  $m$  of lines leaving the  $\Theta_2$  vertex is  $l = m - 1$ . Such diagrams, proportional to  $n^2 (n\tilde{t})^{m-2}$ , are exhausted by the types shown in parts c, d, and e of Fig. 1 (in part e with any number of

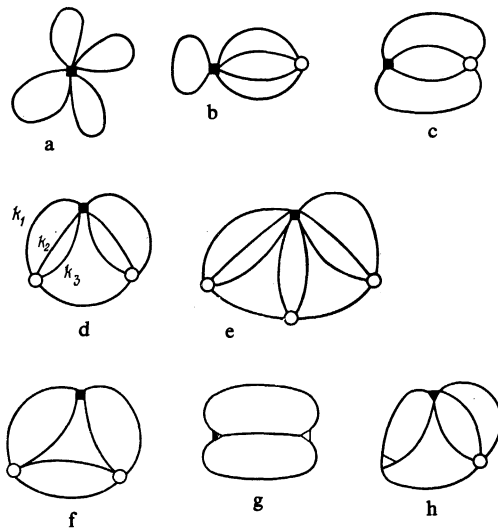


FIG. 1. Examples of multiloop diagrams: the filled and open squares, triangles, and circles denote vertices  $\Theta_2(F_2)$ ,  $\Theta_1(F_1)$ ,  $\Theta_0(F_0')$ , respectively (see Appendix 2).

vertices  $F_0'$ ; it is essential only that any two adjacent  $F_0'$  vertices can be drawn together along a single line; then one vertex and one line vanish, i.e., the number of loops does not change). However, even these diagrams do not contribute to the Gell-Mann–Low equations.

To see this, let us first consider the momentum structure of diagram c. The vertex  $F_0'$  contains two gradients of the fast variable. Symmetrizing the corresponding scalar product by a relabeling of the momenta and using the identity

$$2 \sum_{i \neq j}^l k_i k_j = \left( \sum_{i=1}^l k_i \right)^2 - \sum_{i=1}^l k_i^2, \quad (\text{A.25})$$

we see that the momentum structure reduces to the standard structure

$$\prod_{i=1}^l k_i^{-2}.$$

Consequently, evaluating this diagram with the aid of dimensional regularization<sup>10,11</sup> does not give rise to any important dependence on  $d$ : this diagram is proportional to  $\varepsilon^{-1}$  (where  $\omega = 2 - d > 0$ ) and, just as in a and b, should cancel with the contribution from diagrams of lower orders (since no term  $\propto \varepsilon^{-1}$ , the only one that can contribute to the function  $\beta$ , arises here).

Analogous arguments can also be made for diagrams d and e. Let us arrange the momenta appearing in the last vertex  $F_0'$  as in Fig. 1d. Here these momenta appear in other parts of the diagram only in the form of a sum. Therefore, any linear substitution of the momentum variables which leaves the sum unchanged will not affect the other vertices of the diagram. It is easy to see that such substitutions will permit one to symmetrize the scalar product of momenta at the vertex  $F_0'$  so as to cancel  $(\sum \mathbf{k})^2$  in the denominator of

diagram d after using identity (A.25). As a result, the momentum structure of diagram d reduces to that of diagram c. By repeating this procedure the required number of times, one can also reduce any diagram of type e to form c. (These diagrams are contractible not only in the graphical but also in an analytical sense!) Thus, like diagrams c, all diagrams of types d and e give no contribution to the Gell-Mann–Low equation.

Diagrams of type f, in which the vertices  $F'_0$  are joined by more than two lines, are not trivially reducible. However, for a fixed number of lines leaving the  $\Theta_2$  vertex, these diagrams contain at least one extra loop (in comparison with diagrams c–e): for  $m \ll n$  they are proportional to  $n^m \tilde{t}^{m-1} = n^2(n\tilde{t})^{m-2} \tilde{t}$ . Consequently, the contribution of these diagrams to the RG equations for charges with indices  $n \gtrsim \tilde{t}^{-1}$ , for which the single-loop result (20) gives an unbounded growth, can be neglected in comparison with the single-loop contribution. We stress that the number of such diagrams is finite (i.e., a nonanalytic function  $f(\tilde{t})$  cannot arise), since for a large number of loops ( $m \gg n$ ) the expression  $C_{m+n} \tilde{t}^m$  goes to zero for fixed  $n \sim \tilde{t}^{-1}$ .

Diagrams g and h, which correspond to the second term in (A.24), are outwardly analogous to diagrams c and d, but are nevertheless known to be reducible. This is because the average over angles of the gradients of the slow variables appearing here in different vertices gives rise to a factor  $d^{-1}$  whose expansion contains all powers of  $\varepsilon = 2 - d$ . But because the  $n$  dependence of vertex  $\Theta_1$  for  $m \ll n$  is  $n^{m-1}$  (see above), the contribution of these diagrams to the RG equations goes as  $n^2(n\tilde{t})^{m-3} \tilde{t}$ . Finally, it is easy to see that the most dangerous diagrams, which correspond to the third and fourth terms in (A.24), are proportional to  $n^2(n\tilde{t})^{m-4} \tilde{t}^2$  and  $n^2(n\tilde{t})^{m-4} \tilde{t}^3$ , respectively, i.e., their contribution to the RG equations for charges with indices  $n \sim \tilde{t}^{-1}$  is also negligible.

The RG equations are nevertheless nonlinear even when corrections (A.23) and (A.24) are neglected. The nonlinearity is due to the contribution of charges  $\Gamma$  to the RG equation for  $\tilde{t}$  (A.11); allowance for this contribution makes parametrization (18) inapplicable. Because the bare value of  $\Gamma$  is small, this contribution is negligible for  $\tilde{t}_0 \xi \rightarrow 0$ . It can, however, become relevant even at small  $\Gamma$ , making RG equation (6) for  $\tilde{t}$  formally inapplicable.

<sup>1)</sup>We are considering the replica limit ( $N = 0$ ) of the  $\sigma$  model obtained by integrating over the intermediate fermion fields.<sup>5</sup> The replica limit of the  $\sigma$  model obtained by integrating over the boson fields<sup>6,7,9</sup> or the supersymmetry  $\sigma$  model<sup>10,11</sup> describe the same initial physical model. All of our results would remain unchanged if an alternative  $\sigma$ -model description were chosen.

<sup>2)</sup>The coefficients in vertices (8) and (9) are written in such a way that for the two-dimensional case ( $d = 2$ ) the charges  $\gamma$  and  $\Gamma$  are dimensionless and have a normal scaling dimensionality of zero.

<sup>3)</sup>The vertices obtained on expanding to higher powers of  $k^2$  are unimportant: their normal scale dimensionality at  $d = 2$  is negative. Physically, the difference between the  $\omega$  and  $k$  expansions stems from the fact that in elastic scattering, which leads to quantum interference, the frequency transfer is conserved but the momentum transfer is not.

<sup>4)</sup>The coefficient matrix of the RG equations for charges  $\Gamma_{n_3}$  (9c) has a higher dimensionality than  $D^{(n)}$  for  $n > 4$ , but it contains  $D^{(n)}$  (and consequently,  $C^{(n)}$ ) as a diagonal block, with the additional eigenvalues having a negative real part. For charges  $\Gamma_{n_2}$  (9b) the RG equations coincide for  $\alpha = 0$  with the equations for the charges  $\Gamma_{n_3}$  (9c); for  $\alpha^2 = 1$  the law for the maximum eigenvalue  $\lambda_{\max}$  corresponding to  $\Gamma_{n_2}$  differs unimportantly from (20), but  $\lambda_{\max} \sim n^2$  for  $n > 1$ .

<sup>5)</sup>We are indebted to V. V. Lebedev for suggesting the idea of the proof.

<sup>1</sup>E. Abrahams, P. W. Anderson, D. C. Licciardello, and T. V. Ramakrishnan, Phys. Rev. Lett. **42**, 673 (1979).

<sup>2</sup>N. F. Mott, Adv. Phys. **16**, 49 (1967); Philos. Mag. **29**, 613 (1974).

<sup>3</sup>D. J. Thouless, Phys. Rep. C **13**, 93 (1974); Phys. Rev. Lett. **39**, 1169 (1969).

<sup>4</sup>F. Wegner, Z. Phys. B **35**, 207 (1979).

<sup>5</sup>K. B. Efetov, A. I. Larkin, and D. E. Khmel'nitskiĭ, Zh. Eksp. Teor. Fiz. **79**, 1120 (1980) [Sov. Phys. JETP **52**, 568 (1980)].

<sup>6</sup>L. Schäfer and F. Wegner, Z. Phys. B **38**, 113 (1980).

<sup>7</sup>A. Houghton, A. Jevicki, R. D. Kenway, and A. M. M. Pruisken, Phys. Rev. Lett. **45**, 394 (1980).

<sup>8</sup>S. Hikami, Phys. Rev. B **24**, 2671 (1981).

<sup>9</sup>L. Schäfer and A. M. M. Pruisken, Nucl. Phys. B **200**, 20 (1982).

<sup>10</sup>K. B. Efetov, Zh. Eksp. Teor. Fiz. **82**, 872 (1982) [Sov. Phys. JETP **55**, 514 (1982)].

<sup>11</sup>K. B. Efetov, Adv. Phys. **32**, 53 (1983).

<sup>12</sup>E. Brezin, S. Hikami, and J. Zinn-Justin, Nucl. Phys. B **165**, 528 (1980).

<sup>13</sup>L. P. Gor'kov, A. I. Larkin, and D. E. Khmel'nitskiĭ, Pis'ma Zh. Eksp. Teor. Fiz. **30**, 248 (1979) [JETP Lett. **30**, 228 (1979)].

<sup>14</sup>A. M. Polyakov, Phys. Lett. B **59**, 79 (1975).

<sup>15</sup>H. Eichenherr, Nucl. Phys. B **176**, 223 (1978).

<sup>16</sup>K. B. Efetov, Pis'ma Zh. Eksp. Teor. Fiz. **40**, 17 (1984) [JETP Lett. **49**, 738 (1984)].

<sup>17</sup>S. Edwards and P. W. Anderson, J. Phys. F **5**, 965 (1975).

<sup>18</sup>V. E. Kravtsov and I. V. Lerner, Zh. Eksp. Teor. Fiz. **86**, 1332 (1984) [Sov. Phys. JETP **59**, 778 (1984)].

<sup>19</sup>B. A. Dubrovin, S. P. Novikov, and A. T. Fomenko, Sovremennaya Geometriya [Modern Geometry], Part II, Nauka, Moscow (1979), Secs. 2, 5.

<sup>20</sup>V. E. Kravtsov and I. V. Lerner, Solid State Commun. **52**, 593 (1984).

Translated by Steve Torstveit